



OPEN

Depiction of mosaic perfusion in chronic thromboembolic pulmonary hypertension (CTEPH) on C-arm computed tomography compared to computed tomography pulmonary angiogram (CTPA)

Sabine K. Maschke¹, Thomas Werncke¹, Cornelia L. A. Dewald¹, Lena S. Becker¹, Timo C. Meine¹, Karen M. Olsson², Marius M. Hoepfer², Frank K. Wacker¹, Bernhard C. Meyer¹ & Jan B. Hinrichs¹✉

To evaluate mosaic perfusion patterns and vascular lesions in patients with chronic thromboembolic pulmonary hypertension (CTEPH) using C-Arm computed tomography (CACT) compared to computed tomography pulmonary angiography (CTPA). We included 41 patients (18 female; mean age 59.9 ± 18.3 years) with confirmed CTEPH who underwent CACT and CTPA within 21 days (average 5.3 ± 5.2). Two readers (R1; R2) independently evaluated datasets from both imaging techniques for mosaic perfusion patterns and presence of CTEPH-typical vascular lesions. The number of pulmonary arterial segments with typical findings was evaluated and the percentage of affected segments was calculated and categorized: < 25%; 25–49%; 50–75%; > 75% of all pulmonary arterial segments affected by thromboembolic vascular lesions. Inter-observer agreement was calculated for both modalities using the intraclass-correlation-coefficient (ICC). Based on consensus reading the inter-modality agreement (CACT_{cons} vs. CTPA_{cons}) was calculated using the ICC. Inter-observer agreement was excellent for central vascular lesions (ICC > 0.87) and the percentage of affected segments (ICC > 0.76) and good for the perceptibility of mosaic perfusion (ICC > 0.6) and attribution of the pattern of mosaic perfusion (ICC > 0.6) for both readers on CACT and CTPA. Inter-modality agreement was excellent for the perceptibility of mosaic perfusion (ICC = 1), the present perfusion pattern (ICC = 1) and central vascular lesions (ICC = 1). However, inter-modality agreement for the percentage of affected segments was fair (ICC = 0.50), with a greater proportion of identified affected segments on CACT_{cons}. CACT demonstrates a high agreement with CTPA regarding the detection of mosaic perfusion. CACT detects a higher number of peripheral vascular lesions compared to CTPA.

Abbreviations

BPA	Balloon Pulmonary Angioplasty
CACT	C-Arm computed tomography
CTEPH	Chronic thromboembolic pulmonary hypertension
CTPA	Computed tomography pulmonary angiography
DSA	Digital subtraction angiography

¹Department of Diagnostic and Interventional Radiology, Member of the German Center for Lung Research (DZL), Hannover Medical School, Carl-Neuberg-Str. 1, 30625 Hannover, Germany. ²Clinic for Pneumology, Member of the German Center for Lung Research (DZL), Hannover Medical School, Hannover, Germany. ✉email: Hinrichs.jan@mh-hannover.de

ICC	Intraclass-correlation-coefficient
mPAP	Mean pulmonary arterial pressure
PEA	Pulmonary endarterectomy

Chronic thromboembolic pulmonary hypertension (CTEPH) presents one out of five types of pulmonary hypertension¹. In CTEPH, incomplete resolution and consecutive organization of acute pulmonary emboli causes chronic thromboembolic vascular obstruction. Up to 4% of patients who survived one or more episodes of pulmonary embolism develop CTEPH². However, diagnosis of CTEPH and its differentiation to other types of pulmonary hypertension can be challenging³. Besides typical findings on V/Q scintigraphy and in right heart catheterization, the diagnosis of CTEPH requires typical vascular findings in a suitable imaging modality⁴. Computed tomography pulmonary angiography (CTPA) is an established imaging modality to diagnose CTEPH by visualizing CTEPH-typical vascular findings⁴. Unfortunately, a negative CTPA cannot definitively rule out CTEPH as lesions in small, peripheral branches often stay unnoticed⁴⁻⁶. However, mosaic perfusion detected on CTPA, is a frequent secondary diagnostic parameter in patients suffering from CTEPH, even in the absence of vascular lesions, reflecting the severity of perfusion changes due to chronic pulmonary embolism^{3,7,8}.

Therefore, detection of mosaic perfusion on CTPA in patients with known pulmonary hypertension should trigger further diagnostic work-up, typically including digital subtraction angiography (DSA)^{4,4}. C-Arm computed tomography (CACT) of the pulmonary arteries is an alternative 3D imaging modality that combines imaging features typical for DSA and CTPA. It can easily be acquired during the same session as DSA and offers images with a high spatial resolution that can lead to a more comprehensive imaging work-up of patients with suspected CTEPH⁹. As described previously, CACT provides a more detailed depiction of distal thromboembolic lesions when compared to CTPA⁹. The addition of CACT to the DSA workup improves both, diagnosis and detection of CTEPH-typical vascular lesions which is of decisive importance for the determination of the most suitable treatment option^{3,9-11}. However, the perceptibility of mosaic perfusion on CACT has not been evaluated yet, even though it might offer a more comprehensive and functional approach of CTEPH-induced pathologies than detection of vascular lesions alone.

We aimed to evaluate the perceptibility of patterns of mosaic perfusion and peripheral vascular lesions typical for CTEPH on CACT in comparison to CTPA and to determine its diagnostic value for detection of perfusion inhomogeneities of the lung parenchyma.

Material and methods

Our local ethics committee (Ethics committee Hannover Medical School, Hannover, Germany) approved this retrospective study. Informed consent was waived by the same committee. All experiments were performed in accordance with relevant guidelines and regulations. Between June 2013 and July 2020 420 patients (204 female (48.6%), 216 male (51.4%); mean age 59.9 ± 18.3 years) underwent our standardized diagnostic work-up for suspected CTEPH as described elsewhere, including DSA and CACT in our angiographic suit¹². For 54 patients (12.9%) an additional CTPA was available for review in our picture archiving and communication system. Out of these 54 patients, we included 41 (18 female (44%), 23 male (56%)) who met our predefined criteria: 1. confirmed CTEPH according to current guidelines (mean pulmonary arterial pressure (mPAP) 43.5 ± 11.6 mmHg)⁴. 2. additional CTPA, (a) meeting the minimally required image quality criteria according to the American College of Radiology recommendations for computed tomography for the evaluation of pulmonary embolism¹³ and (b) performed within a maximum of 21 days (5.3 ± 5.2 days) to rule out acute pulmonary embolism as the cause of sudden, newly occurred or significantly worsened shortness of breath. However, CTPA could rule out acute pulmonary embolism or pulmonary consolidations.

Parts of the presented study population has been included previously in other studies. However, the perceptibility of parenchymal lung pathologies on CACT compared to CTPA was not the aim of the previous studies. For patient demographics see Table 1.

CACT. All procedures were performed on a monoplane, ceiling-mounted angiographic system (Artis Q, Siemens Healthineers, Forchheim, Germany) or on a monoplane, robotic-arm-mounted angiographic system (Artis pheno, Siemens Healthineers, Forchheim, Germany). A 5 F pigtail catheter (Cordis, Waterloo, Belgium) was placed in the pulmonary trunk. CACT was obtained using the manufacturer's preset during contrast injection (total injected volume 70 mL, comprising 49 mL Iomeprol 300 mgI/mL and 21 mL saline, effective iodine concentration 210 mgI/mL, flow rate 8 mL/s) within a single modest breath hold as described previously¹². In order to optimize the anatomical coverage, the field of view was centered on the central pulmonary arteries under fluoroscopic control.

CTPA. We included 41 contrast-enhanced multidetector CTPA. 32 (78.0%) were performed at our institution and 9 (22.0%) performed outside of our hospital. All images were available for review in our picture archiving and communication system.

To address potential heterogeneity of the images, we defined minimally required image quality criteria according to the American College of Radiology recommendations for computed tomography for the evaluation of pulmonary embolism¹³. In brief: CTPA were performed on a multidetector-row CT to detect pulmonary embolism, using automated bolus tracking in the main pulmonary artery and automated contrast material injection with a flow rate of 3 mL per second, with a slice thickness of ≤ 1.5 mm and acquired within a maximum of 21 days prior to or past CACT. The mean slice thickness was 1.26 ± 0.31 mm, the mean period between CACT and CTPA acquisition measured 5.3 ± 5.2 days. 11 CTPA (26.8%) were performed after previous CACT, 30 CTPA (73.2%) afterwards.

Age	59.9 ± 18.4
Sex (n, %)	18 female (44), 23 male (56)
mPAP (mmHg)	43.5 ± 11.6 mmHg
Treatment	
Balloon pulmonary angioplasty	8 (19.5)
Pulmonary endarterectomy	33 (80.5)

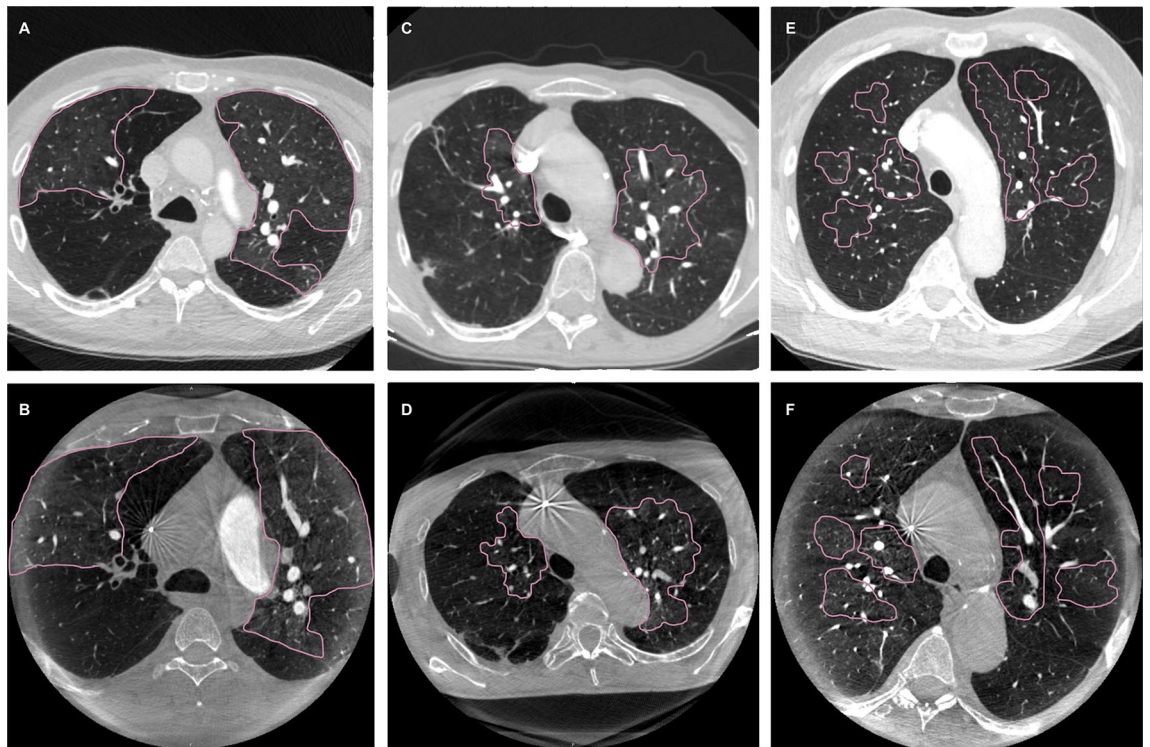
Table 1. Patient characteristics.**Figure 1.** Patterns of mosaic perfusion on CT and CACT. (A, B) pattern 1, sharply demarcated segmental and/or subsegmental areas of hypo- and hyperattenuation with well-defined borders corresponding to the anatomic unit of the secondary pulmonary lobule on CT (A) and CACT (B); (C, D) pattern 2, perihilar hyperattenuating areas with peripheral perfusion defects on CT (C) and CACT (D); (E, F) pattern 3, diffuse heterogeneity of lung attenuation with patchy low-attenuating areas located more centrally within in the secondary lobule and intermixed with areas of normal or increased attenuation on CT (E) and CACT (F).

Image analysis. During two separate sessions and in random order of patients, two readers with 5 and 9 years (R1: S.K.M.; R2: J.B.H.) of clinical experience in cardiovascular and interventional imaging independently reviewed anonymized images of both modalities. The CACT images were analyzed during a first session and the CTPA images during a second session as described previously¹². CACT and CTPA were reviewed regarding three categories: First, the presence of mosaic perfusion was assessed. If present, mosaic perfusion was divided into three patterns according to Grosse et al.: pattern 1, sharply demarcated segmental and/or subsegmental areas of hypo- and hyperattenuation with well-defined borders corresponding to the anatomic unit of the secondary pulmonary lobule; pattern 2, perihilar hyperattenuating areas with peripheral perfusion defects; and pattern 3, diffuse heterogeneity of lung attenuation with patchy low-attenuating areas located more centrally within in the secondary lobule and intermixed with areas of normal or increased attenuation¹⁴ (Fig. 1). Second, thromboembolic vascular findings typical for CTEPH were assessed: stenosis, wall-adherent thrombi, intraluminal structures, abrupt narrowing, complete obstruction on central (central pulmonary artery to segmental pulmonary arteries) or peripheral (sub-segmental) levels of the pulmonary vascular tree. Third, the number of pulmonary arterial segments with findings typical for CTEPH was evaluated. Accordingly, the percentage of affected segments was calculated and categorized as follows: < 25%; 25–49%; 50–75%; > 75% of all pulmonary arterial segments are affected by thromboembolic pathologies typical for CTEPH.

	R1:R2 CTPA	R1:R2 CACT
Perceptibility of mosaic perfusion (ICC)	0.66 (0.44–0.80)	0.66 (0.45–0.80)
Perceptibility of central vascular lesions (ICC)	0.88 (0.78–0.93)	0.88 (0.78–0.93)
Percentage of affected segments (ICC)	0.92 (0.84–0.95)	0.77 (0.61–0.87)
Attribution of the pattern of mosaic perfusion (ICC)	0.61 (0.38–0.78)	0.61 (0.37–0.77)

Table 2. Inter-observer agreement between Reader 1 (R1) and Reader 2 (R2).

	CTPA _{cons} :CACT _{cons}
Perceptibility of mosaic perfusion (ICC)	1 (1.0–1.0)
Perceptibility of central vascular lesions (ICC)	1 (1.0–1.0)
Percentage of affected segments (ICC)	0.5 (0.01–0.76) ***
Attribution of the pattern of mosaic perfusion (ICC)	1 (1.0–1.0)

Table 3. Inter-modality agreement between CTPA_{cons} and CACT_{cons}. *** $p < 0.001$, values are given in mean with 95% confidence interval, as the ICC for any other parameter is 1, no p-Values are given.

Data evaluation. Inter-observer agreement for CACT and CTPA was calculated for all three categories. Subsequently, a CACT consensus (CACT_{cons}) and a CTPA consensus (CTPA_{cons}) were created based on the documented findings of both readers. If there was disagreement, the images were re-assessed by both readers together in order to reach a consensus. Finally, inter-modality agreement for CACT_{cons} and CTPA_{cons} was calculated.

Statistical analysis. Descriptive statistical analyses of the patient demographics were calculated (mean value \pm standard deviation). Inter-observer and inter-modality agreement of all categories were determined by using the intraclass-correlation-coefficient (ICC). The following classification was used for interpretation: poor (< 0.40); fair (0.4–0.59); good (0.6–0.74); excellent (≥ 0.75)¹⁵. Statistical analysis was conducted with R (version 3.6.1, <http://www.r-project.org> with package “IRR” version 0.84.1).

Results

Inter-observer agreement. Inter-observer agreement between R1 and R2 was excellent for the perceptibility of central vascular lesions (CTPA: ICC = 0.88, CACT: ICC = 0.88) and the percentage of affected segments (CTPA: ICC = 0.92, CACT: ICC = 0.77). Inter-observer agreement was good for the perceptibility of mosaic perfusion (CTPA: ICC = 0.66, CACT: ICC = 0.66) and attribution of the pattern of mosaic perfusion (CTPA: ICC = 0.62, CACT: ICC = 0.61; also refer to Table 2).

Inter-modality agreement. After conducting a consensus reading, CACT_{cons} and CTPA_{cons} were used to calculate inter-modality agreement. Inter-modality agreement between CACT_{cons} and CTPA_{cons} for the perceptibility of mosaic perfusion was excellent (ICC = 1): with both modalities, mosaic perfusion was present in 40 patients (97.6%), in 1 patient (2.4%) it was not. The inter-modality agreement for the attribution of the pattern of mosaic perfusion was also excellent (ICC = 1): on both modalities, pattern 1 occurred in 28 patients (68.3%), pattern 2 in 7 patients (17.1%) and pattern 3 in 5 patients (12.2%; Table 3). Furthermore, inter-modality agreement for the perceptibility of central vascular lesions was also excellent (ICC = 1): on both modalities, 29 patients (70.7%) showed central lesions, 12 (29.3%) did not (Fig. 2). However, inter-modality agreement for the percentage of affected segments was fair (ICC = 0.50) with an overall higher percentage of pulmonary arterial segments displaying intravascular lesions typical for CTEPH on CACT compared to CTPA (p -Value < 0.001). On CACT no patient (0%) showed less than 25% of affected segments, 1 patient (2.4%) 25–49%, 5 patients (12.2%) 50–75% and 35 patients (85.4%) more than 75%. Though, on CTPA 2 patients (4.9%) showed less than 25% of segments affected, 3 patients (7.3%) 25–49%, 16 patients (39.0%) 50–75% and 20 patients (48.8%) more than 75%.

Discussion

CACT and CTPA yielded excellent agreement for the diagnosis of mosaic perfusion and the detection of different perfusion patterns. Furthermore, the number of pulmonary arterial segments with intravascular lesions typical for CTEPH was higher with CACT compared to CTPA. Although there was no gold standard, the higher number of CTEPH-typical findings detected by CACT in combination with the visualization of mosaic perfusion emphasizes the added value of CACT in the diagnostic work-up of patients with CTEPH.

The depiction of peripheral web-like stenoses, intraluminal bands and total occlusions in segmental and sub-segmental pulmonary arteries is of high significance in the diagnostic work-up of patients with suspected CTEPH, as this might be a decisive criterion for both, final diagnosis and therapeutic decision^{4,16}. However, especially in patients with predominantly distal thromboembolic lesions, secondary signs are a valuable diagnostic criteria for CTEPH when using CTPA as initial imaging modality⁴. It has been shown that segmental vessel size disparity, mosaic perfusion, enlarged bronchial arteries and bronchial dilatation can be used to reliably

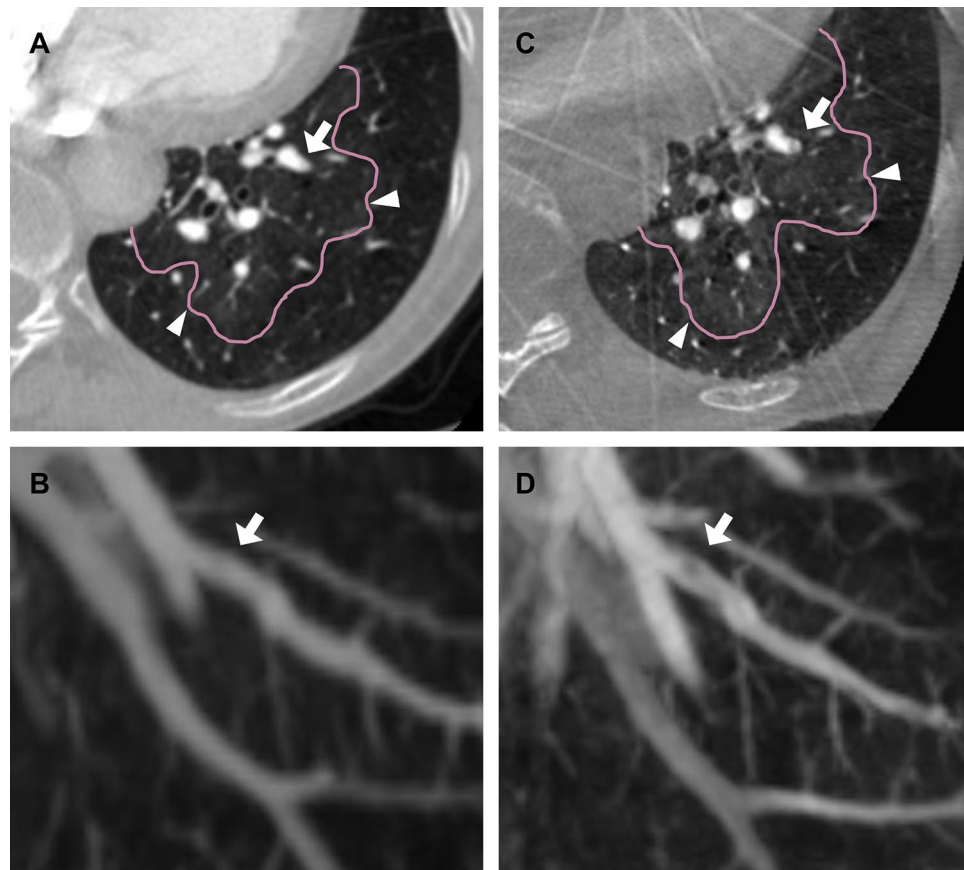


Figure 2. Depiction of peripheral intravascular lesions on CT and CACT. (A, C) axial multiplanar reformation of the left lower lobe shows mosaic perfusion (arrow heads) on CTPA (A) and CACT (C). (B, D) corresponding 20 mm maximal intensity projection of CTPA (B) and CACT (D) reveals an intravascular band in pulmonary artery segment VIII (arrow) as a typical finding for CTEPH on CACT (D) but not on CTPA (B).

distinguish CTEPH from other clinical groups of pulmonary hypertension³. Among these, mosaic perfusion, as a sign of perfusion irregularities, is an important criterion to confirm pulmonary hypertension caused by thromboembolic vascular alterations³. Therefore, mosaic perfusion on CTPA, even in the absence of vascular findings, should trigger a dedicated diagnostic work-up which usually includes DSA as the imaging modality of choice.

In this context, CACT is a reasonable addition in the diagnostic work-up of patients with suspected CTEPH. As the development of digital, flat-panel detector angiographic systems with high frame rates enabled three dimensional tomographic reconstructions by combining valuable imaging characteristics from both, DSA and CTPA, CACT can easily be combined with acquisition of DSA during one session in the angiographic suite^{17–19}. Local administration of contrast agent in the main pulmonary artery can compensate the, compared to multi detector CT, slightly inferior contrast and temporal resolution, as it results in an exclusive and strong enhancement of the pulmonary arteries, enabling an excellent arterial and venous phase separation, facilitating the identification of distal thromboembolic lesions^{1,9,10,17–19}. Altogether offering a three dimensional data set with high spatial resolution of peripheral, subsegmental intravascular lesions as well as additional information regarding the vascular wall, adjacent bronchi and the surrounding tissue^{1,9,10}. Previous studies confirmed that CACT is superior in visualizing intravascular lesions in the subsegmental pulmonary arteries compared to conventional DSA and CTPA^{10,11}. This is reflected in our study by the higher number of affected segments recognized on CACT. In addition, mosaic perfusion, a marker for regional perfusion differences can also be detected by CACT which has not been evaluated so far. This might be of value to assess the extent and characteristics of microperfusion defects.

However, when evaluating its applicability and possible benefits, it needs to be considered that CACT causes additional radiation exposure and additional need for contrast media. The effective radiation dose of thoracic CACT is comparable to that of multi detector CT¹⁰. The average amount of contrast media required for the assessment of the pulmonary arteries using newest CT scanners is 80 mL and thus, approximately twice as much as is usually used in CACT^{12,20,21}. This has to be balanced out with the advantages of CACT, which facilitates the detection of mosaic perfusion and the distinction of different patterns equivalent to CTPA combined with a superior depiction of peripheral vascular lesions¹².

Sherrick et al. showed that mosaic attenuation due to perfusion irregularities has a significantly higher frequency in patients with pulmonary hypertension due to vascular disease. However, the authors did not clarify how many patients with CTEPH showed mosaic perfusion, as they did not discriminate chronic or acute pulmonary embolism as cause for pulmonary hypertension⁸. Furthermore, Bergin et al. described mosaic perfusion in

combination with segmental vessel size disparity to be highly specific for CTEPH. However, the true prevalence of mosaic perfusion in the study population remains unclear as the authors did not distinguish between mosaic attenuation due to infiltrative lung or small airways disease and mosaic attenuation due to occlusive vascular disease⁷.

In 2017, Grosse et al. evaluated prevalence of vascular and parenchymal lung pathologies on CTPA in patients with different causes of pulmonary hypertension to determine secondary diagnostic signs for differentiating CTEPH from non-thromboembolic pulmonary hypertension³. Both, vascular and parenchymal CT findings were useful to differentiate between CTEPH and other forms of pulmonary hypertension. Furthermore, they found that a combination of mosaic perfusion and segmental vessel size disparity was highly specific for CTEPH, whereas mosaic perfusion alone also frequently appeared in pulmonary arterial hypertension³.

In an additional study, Grosse et al. evaluated CT imaging findings in patients newly diagnosed with CTEPH. They surveyed the frequency of mosaic perfusion and distinguished between different patterns of mosaic perfusion and their incidence. Mosaic perfusion occurred with a frequency of 92.1%. Accordingly, we observed mosaic perfusion in 97.6% of patients. Perfusion pattern 1 also was the most frequent (68.3%) in our study, followed by pattern 2 (17.1%) and pattern 3 (12.2%). Furthermore, Grosse et al. reported a significantly higher frequency of mosaic perfusion in patients with peripheral pulmonary embolism in comparison to patients with exclusively central thromboembolic lesions¹⁴. In our study, all patients showed peripheral thromboembolic lesions. This finding might explain the even higher incidence of mosaic perfusion in our study compared to the results of Grosse et al.

In patients with CTEPH, areas of hyperattenuation are most likely caused by local hyperperfusion^{7,16,22}: it has been shown that systemic blood flow to the lung increases significantly after acute pulmonary embolism and increases even further in patients with CTEPH^{5,6,23,24}. The extent of systemic collateral perfusion is a well-known, valid prognostic factor for postsurgical outcome after pulmonary endarterectomy²⁵. The occurrence and characteristics of mosaic perfusion, as they indirectly reflect the severity of perfusion impairment, can be used to estimate the dimension of systemic collateral perfusion, hence possibly serving as a tool to estimate the therapeutic benefit. However, Oikonomou et al. did not find a connection between the presence of mosaic perfusion and postoperative outcome after pulmonary endarterectomy (PEA)²⁵. Though, the outcome, as measured by decrease of mean pulmonary arterial pressure, was estimated shortly after the surgery, when removing the peri-operative Swan Ganz catheter and transferring the patients from Intensive Care Unit²⁵. It is possible, that microvascular changes prior to therapy might take longer to show significant improvement. Therefore, an additional follow up at a later date seems reasonable.

Therefore, its reliable depiction on CACT once more emphasizes the value of CACT in the diagnostic work-up of patients with suspected CTEPH: CACT not only enables improved detection of vascular lesions compared to CTPA or DSA but additionally also offers a more functional approach of CTEPH-induced pathologies than detection of vascular lesions alone, something unachievable with DSA alone.

Our study has several limitations. First, CACT and CTPA have not been acquired at the same day. However, patients did not undergo therapeutic interventions during the interval between both examinations and we did not find differences regarding the presence and pattern of mosaic perfusion on both modalities. Second, CTPA has been acquired on different scanners and with slightly different protocols. Though, we defined the minimum required image quality criteria to ensure comparability. A correlation of histologic probes with the peripheral vascular lesions only detected on CACT and possibly treatable with BPA is impossible as no thromboembolic material is removed during the procedure. Therefore, a gold standard and terminal proof cannot be carried out. Furthermore, our study was done at a single institution with a relatively small number of patients.

Conclusion

CACT demonstrates a high agreement with CTPA regarding the detection of mosaic perfusion and the distinction of different mosaic perfusion patterns in patients with CTEPH. CACT detects a higher number of peripheral vascular lesions compared to CTPA, indicating the value of additional CACT in the diagnostic work-up of patients with CTEPH eligible for surgery or balloon pulmonary angioplasty (BPA).

Received: 11 June 2021; Accepted: 23 September 2021

Published online: 08 October 2021

References

1. Galiè, N. et al. 2015 ESC/ERS Guidelines for the diagnosis and treatment of pulmonary hypertension: The joint task force for the diagnosis and treatment of pulmonary hypertension of the European society of cardiology (ESC) and the European respiratory society (ERS): Endorsed by: Association for European paediatric and congenital cardiology (AEPC), international society for heart and lung transplantation (ISHLT). *Eur. Heart J.* **37**, 67–119 (2016).
2. Pengo, V. et al. Incidence of chronic thromboembolic pulmonary hypertension after pulmonary embolism. *N Engl. J. Med.* **350**, 2257–2264 (2004).
3. Grosse, A., Grosse, C. & Lang, I. M. Distinguishing chronic thromboembolic pulmonary hypertension from other causes of pulmonary hypertension using CT. *AJR Am. J. Roentgenol.* **209**, 1228–1238 (2017).
4. Wilkens, H. et al. bChronic thromboembolic pulmonary hypertension (CTEPH): Updated recommendations from the cologne consensus conference 2018. *Int. J. Cardiol.* **272S**, 69–78 (2018).
5. Mitzner, W. & Wagner, E. M. Vascular remodeling in the circulations of the lung. *J. Appl. Physiol.* **1985**(97), 1999–2004 (2004).
6. Shimizu, H. et al. Dilatation of bronchial arteries correlates with extent of central disease in patients with chronic thromboembolic pulmonary hypertension. *Circ. J.* **72**, 1136–1141 (2008).
7. Bergin, C. J. et al. Accuracy of high-resolution CT in identifying chronic pulmonary thromboembolic disease. *AJR Am. J. Roentgenol.* **166**, 1371–1377 (1996).
8. Sherrick, A. D., Swensen, S. J. & Hartman, T. E. Mosaic pattern of lung attenuation on CT scans: Frequency among patients with pulmonary artery hypertension of different causes. *AJR Am. J. Roentgenol.* **169**, 79–82 (1997).

9. Hinrichs, J. B. *et al.* Pulmonary artery imaging in patients with chronic thromboembolic pulmonary hypertension: Comparison of cone-beam CT and 64-row multidetector CT. *J. Vasc. Int. Radiol.* **27**, 361–8.e2 (2016).
10. Hinrichs, J. B. *et al.* Comparison of C-arm computed tomography and digital subtraction angiography in patients with chronic thromboembolic pulmonary hypertension. *Cardiovasc. Int. Radiol.* **39**, 53–63 (2016).
11. Maschke, S. K. *et al.* C-Arm computed tomography (CACT)-guided balloon pulmonary angioplasty (BPA): Evaluation of patient safety and peri- and post-procedural complications. *Eur. Radiol.* **29**, 1276–1284 (2019).
12. Maschke, S.K., *et al.* The value of C-Arm computed tomography in addition to conventional digital subtraction angiography in the diagnostic work-up of patients with suspected chronic thromboembolic pulmonary hypertension: An update of 300 patients. *Acad Radiol.* S1076–6332(20)30421–9. [published online ahead of print, 2020 Aug 4]. (2020)
13. American College of Radiology. ACR–NASCI–SIR–SPR practice parameter for the performance and interpretation of body computed tomography angiography (CTA). (2017)
14. Grosse, A., Grosse, C. & Lang, I. Evaluation of the CT imaging findings in patients newly diagnosed with chronic thromboembolic pulmonary hypertension. *PLoS ONE* **13**, e0201468 (2018).
15. Cicchetti, D. V. Guidelines, criteria, and rules of thumb for evaluating normed and standardized assessment instruments in psychology. *Psychol. Assess.* **6**, 284–290 (1994).
16. Olsson, K. M. *et al.* Chronic thromboembolic pulmonary hypertension. *Dtsch Arztebl Int.* **111**, 856–862 (2014).
17. Meyer, B. C. *et al.* Visualization of hyper-vascular liver lesions during TACE: COMPARISON of angiographic C-arm CT and MDCT. *Am. J. Roentgenol.* **190**, W263–269 (2008).
18. Fahrig, R. *et al.* Dose and image quality for a cone-beam C-arm CT system. *Med. Phys.* **33**, 4541–4550 (2006).
19. Meyer, B. C. *et al.* Contrast-enhanced abdominal angiographic CT for Intra-abdominal tumor embolization: A new tool for vessel and soft tissue visualization. *Cardiovasc. Int. Radiol.* **30**, 743–749 (2007).
20. Singh, R. *et al.* Quantitative lobar pulmonary perfusion assessment on dual-energy CT pulmonary angiography: Applications in pulmonary embolism. *Eur. Radiol.* **30**, 2535–2542 (2020).
21. Sugiura, T. *et al.* Role of 320-slice CT imaging in the diagnostic workup of patients with chronic thromboembolic pulmonary hypertension. *Chest* **143**, 1070–1077 (2013).
22. McCann, C., Gopalan, D., Sheares, K. & Screatton, N. Imaging in pulmonary hypertension, part 2: Large vessel diseases. *Postgrad Med. J.* **88**, 317–325 (2012).
23. Michel, R. P. & Hakim, T. S. Increased resistance in postobstructive pulmonary vasculopathy: Structure-function relationships. *J. Appl. Physiol.* **1985**(71), 601–610 (1991).
24. Remy-Jardin, M. *et al.* Systemic collateral supply in patients with chronic thromboembolic and primary pulmonary hypertension: Assessment with multi-detector row helical CT angiography. *Radiology* **235**, 274–281 (2005).
25. Oikonomou, A. *et al.* Chronic thromboembolic pulmonary arterial hypertension: Correlation of postoperative results of thromboendarterectomy with preoperative helical contrast-enhanced computed tomography. *J. Thorac. Imaging.* **19**, 67–73 (2004).

Author contributions

All authors of this work contributed substantially to conception and design, data acquisition, or analysis and interpretation of data. All authors drafted or revised the article for important intellectual content and approved the final version of the manuscript.

Funding

Open Access funding enabled and organized by Projekt DEAL. The study was funded in parts by personal grants from the “Junge Akademie” and PRACTIS (Program of Hannover Medical School for Clinician Scientists).

Competing interests

The authors declare no competing interests.

Additional information

Correspondence and requests for materials should be addressed to J.B.H.

Reprints and permissions information is available at www.nature.com/reprints.

Publisher’s note Springer Nature remains neutral with regard to jurisdictional claims in published maps and institutional affiliations.



Open Access This article is licensed under a Creative Commons Attribution 4.0 International License, which permits use, sharing, adaptation, distribution and reproduction in any medium or format, as long as you give appropriate credit to the original author(s) and the source, provide a link to the Creative Commons licence, and indicate if changes were made. The images or other third party material in this article are included in the article’s Creative Commons licence, unless indicated otherwise in a credit line to the material. If material is not included in the article’s Creative Commons licence and your intended use is not permitted by statutory regulation or exceeds the permitted use, you will need to obtain permission directly from the copyright holder. To view a copy of this licence, visit <http://creativecommons.org/licenses/by/4.0/>.

© The Author(s) 2021